

This is the accepted manuscript made available via CHORUS. The article has been published as:

## Specific heat of $\text{Nd}_{1-x}\text{Ca}_x\text{B}_6$ single crystals

Jolanta Stankiewicz, Marco Evangelisti, and Zachary Fisk

Phys. Rev. B **83**, 113108 — Published 29 March 2011

DOI: [10.1103/PhysRevB.83.113108](https://doi.org/10.1103/PhysRevB.83.113108)

# Specific heat of $\text{Nd}_{1-x}\text{Ca}_x\text{B}_6$ single crystals

Jolanta Stankiewicz,<sup>1,\*</sup> Marco Evangelisti,<sup>1</sup> and Zachary Fisk<sup>2</sup>

<sup>1</sup>*Instituto de Ciencia de Materiales de Aragón and  
Departamento de Física de la Materia Condensada,  
CSIC–Universidad de Zaragoza, 50009-Zaragoza, Spain*

<sup>2</sup>*Department of Physics, University of California, Irvine in Irvine, CA 92697, USA*

(Dated: January 25, 2011)

We measured the heat capacity on random alloys of  $\text{Nd}_{1-x}\text{Ca}_x\text{B}_6$  ( $x < 0.4$ ) in the 0.4 to 300 K temperature range. We calculated the lattice contribution to the specific heat, arising from the Debye-type phonons of the boron framework and Einstein-type oscillators of the cation sublattice. Subtracting lattice and Schottky-type contributions from the measured heat capacity, we find that the electronic portion, linear in temperature, decreases sharply upon doping with Ca.

PACS numbers: 71.27.+a, 75.40.-s, 65.40.Ba

## I. INTRODUCTION

Rare-earth and alkaline-earth metal hexaborides show unusual physical properties, more so if they are synthesized with divalent cations. Their properties can be altered profoundly by slight variations in the band structure, for instance, through doping. For this reason they have been the subject of extensive experimental and theoretical studies for over four decades. Hexaborides exist in the cubic CsCl crystal structure, in which a cage of  $B_6$  octahedra surrounds each cation atom. Compounds with divalent cations are semiconducting. Trivalent cations give rise to metallicity with an estimated one conduction electron per metal atom. Since the hexaborides with different cations remain isostructural, doping studies have been a major component of the experimental work done on these materials. In addition, the strong interaction between the conduction electrons, at low temperatures, makes this class of materials one of the most interesting in the field of strongly correlated electron systems.

Most of the rare earth hexaborides exhibit some sort of long-range order at low temperatures. The most common is antiferromagnetic (AF) ordering through the Ruderman-Kittel-Kasuya-Yosida (RKKY) exchange interaction, which is strongly influenced by crystal field effects, as is seen in  $NdB_6$ . This compound orders in an  $A$ -type collinear antiferromagnetic (AF) structure below  $T_N \approx 8$  K.<sup>2</sup> The ground state of the  $Nd^{+3}$  ions ( $J = 9/2$ ) is split in a cubic crystal field into two  $\Gamma_8$  quartets and a  $\Gamma_6$  doublet.<sup>3,4</sup> The first excited energy is approximately 135 K above the ground  $\Gamma_8^2$  state, and the nearest  $\Gamma_6$  excited doublet lies at 278 K.<sup>3-5</sup> A competition between ferro-quadrupolar<sup>6</sup> and crystalline-electric field<sup>4</sup> (CEF) interactions gives rise to a low-field magnetic anisotropy in  $NdB_6$  which is much weaker than the isotropic magnetic exchange interaction. The topology of the Fermi surface (FS) of  $NdB_6$  has been explored in several works.<sup>7-9</sup> It resembles the FS observed in  $LaB_6$ ,<sup>10</sup> but with additional weak correlations. The FS consists of six large ellipsoids, centered at the  $X$  points of the Brillouin zone, which slightly overlap on the  $\Gamma MX$  plane. A simple folding procedure can be used to obtain the AF bands from their paramagnetic counterparts in this hexaboride.<sup>11</sup> In addition, the experimentally found frequency branches of the de Haas-van Alphen effect<sup>8</sup> can be well reproduced from the calculated Fermi surfaces.<sup>12</sup> Band structure calculations also show that  $4f$  levels are rather deep in  $NdB_6$ .<sup>13</sup>

Results of experiments on the thermodynamic properties of  $NdB_6$  have been reported in several papers.<sup>5,14-18</sup> Magnetic contributions to the specific heat have been found, subtracting

the results which had been reported for isostructural  $\text{LaB}_6$ . Experimental estimations of the electronic term of the specific heat are scarce and vary from 2 to 80 mJ/K<sup>2</sup>mol.<sup>15,16</sup>

In this paper we report heat capacity measurement results for  $\text{Nd}_{1-x}\text{Ca}_x\text{B}_6$  alloys, in which some of the trivalent rare-earth atoms are substituted with divalent Ca atoms. We aim to study how a decreasing valence, and the variations in the Fermi surface (FS) that follow from it, affect the properties of these alloys. We find that the electronic (linear in temperature) specific heat is moderately enhanced in the paramagnetic region of  $\text{NdB}_6$ . It decreases sharply with increasing the content of Ca for  $x \lesssim 0.1$ .

We describe the experimental procedure in Section II. Results of measurements are reported and discussed in Section III. Conclusions are drawn in Section IV.

## II. EXPERIMENT

Single crystals of  $\text{Nd}_{1-x}\text{Ca}_x\text{B}_6$  with  $x < 0.4$  were grown from stoichiometric amounts of hexaboride components in an Al flux. Crystals grown by this method can often contain flux inclusions or secondary phases within the bulk, or on the surface. We used electron probe analysis to check the composition and homogeneity of the crystals we studied. We found that the Ca and Nd concentrations are spatially uniform over the crystal surfaces. A negligible contamination from Al was seen on some samples. The crystalline structure of alloys was determined by x-ray diffraction.

In our heat capacity experiments, we used small single crystals with an approximate mass of 2 mg. We also measured the heat capacity of a  $\text{LaB}_6$  single crystal for a reference purpose. All measurements were performed in a Quantum Design Physical Properties Measurement System (PPMS), with a  $\text{He}^3$  insert, which enables access to temperatures as low as 0.38 K. A small amount of Apiezon N grease was used in order to hold the crystal in place on a sapphire platform and to assure good thermal contact between the crystal and the platform. The PPMS measures the heat capacity at constant pressure using the relaxation method.

## III. RESULTS AND DISCUSSION

How the zero-field specific heat  $C$ , obtained for several  $\text{Nd}_{1-x}\text{Ca}_x\text{B}_6$  single crystals, varies with temperature  $T$  in the range from 0.4 to 300 K is shown in Fig. 1. The sharp peaks

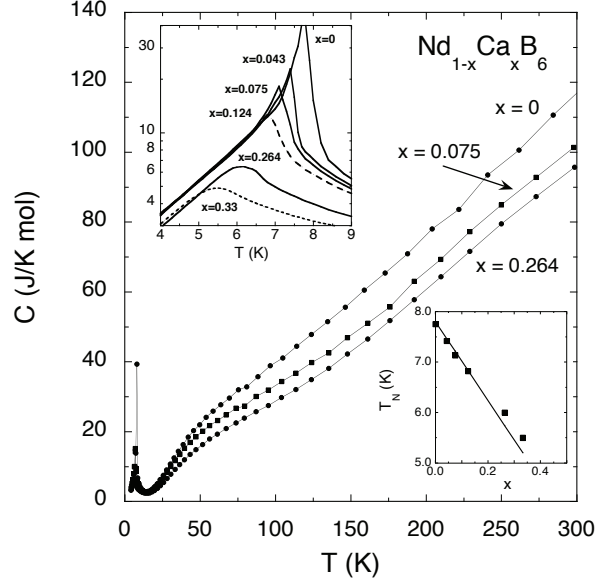


FIG. 1. Plots of  $C$  vs  $T$  for  $\text{Nd}_{1-x}\text{Ca}_x\text{B}_6$  single crystals. A blow up of the transition region is shown in the upper inset. The solid and dashed lines are guides to the eye. The variation of the critical temperature with  $x$  is displayed in the lower inset. The solid line is the expected variation (see text).

in the  $C(T)$  curves come from the antiferromagnetic phase transition; for  $\text{NdB}_6$ ,  $T_N = 7.7$  K. Upon doping with Ca, the peak at  $T_N$  shifts to lower temperatures and becomes smaller with a larger high-temperature tail. This is shown in the inset of Fig. 1. The variation of the critical temperature with  $x$  can easily be explained within the frame of molecular field theory for which  $T_N$  is linearly proportional to the number  $n_{\text{Nd}}$  of nearest magnetic neighbors for each  $\text{Nd}^{3+}$  ion. Since the inclusion of calcium causes a change in  $n_{\text{Nd}}$ , the shift of the ordering temperature is expressed as  $T_N(\text{Nd}_{1-x}\text{Ca}_x\text{B}_6) = (1-x)T_N(\text{NdB}_6)$ . The lower inset of Fig. 1 shows that the agreement between the observed and expected (from the above relation) ordering temperatures is very good.

Generally, there are electronic, magnetic and phonon contributions to the specific heat  $C(T)$ , *i.e.*  $C(T) = C_{el} + C_{mag} + C_{ph}$ . In order to analyze the electronic  $C_{el}$  and magnetic  $C_{mag}$  parts of the specific heat, we need to model and then subtract from the total heat capacity the phonon contribution  $C_{ph}$ . The latter was calculated using a model, first proposed by Mandrus and collaborators<sup>19</sup> for hexaborides, that treats the rare earth or other metal ions as independent harmonic (Einstein) oscillators embedded in a Debye bath of boron ions. This

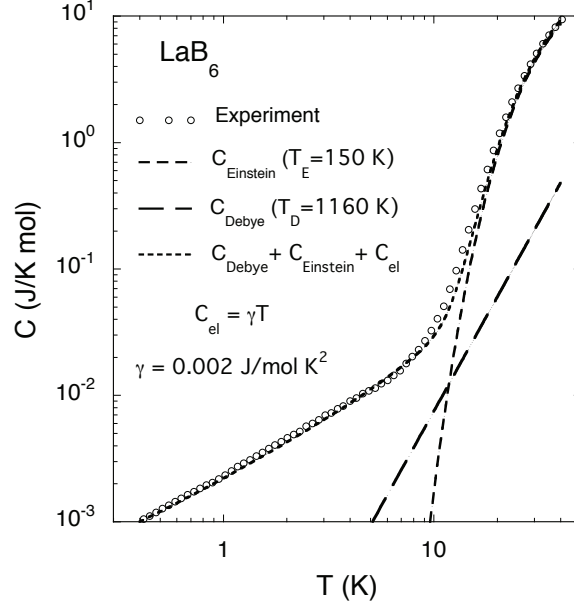


FIG. 2. Specific heat per mole of  $\text{LaB}_6$  vs temperature and model calculations performed as described in the text.

follows from the observation that the metal ions are weakly bound in hexaborides but strong covalent bonds between boron atoms give rise to a very rigid boron sublattice. To check the applicability of this model, we have compared its predictions to the experimental data which we have obtained for the heat capacity of a  $\text{LaB}_6$  single crystal in a temperature range 0.3–40 K. A value of 150 K and of 1160 K has been assumed for the Einstein and Debye's temperature, respectively. These values follow from corresponding atomic displacements parameters.<sup>19</sup> As shown in Fig. 2, the agreement between experimental and calculated heat capacity is nearly perfect, assuming a small electronic term of 0.002 J/mol K<sup>2</sup>.

To proceed with calculations of the phonon contribution in  $\text{Nd}_{1-x}\text{Ca}_x\text{B}_6$  alloys, we estimate Einstein temperature  $T_E$  of the Nd and Ca atoms from their atomic displacement parameters at room temperature.<sup>19–22</sup> We used a value of 150 K and of 280 K for  $T_E$  of Nd and Ca, respectively. These are very close to the values which one obtains by renormalization of  $T_E(\text{La})$  by the square root of the corresponding mass ratio. An examination of x-ray refinements implies a Debye temperature of approximately 1300 K for the simple cubic  $\text{B}_6$  lattice in  $\text{NdB}_6$ .<sup>21</sup> The lattice specific heat is now given by:  $C_{ph} = C_{ph}(\text{Debye}) + xC_{ph}(\text{Einstein}, \text{Ca}) + (1-x)C_{ph}(\text{Einstein}, \text{Nd})$ ; six moles of B ions are treated as a Debye solid and  $1-x$  ( $x$ ) moles of Nd (Ca) ions as Einstein oscillators. How these terms

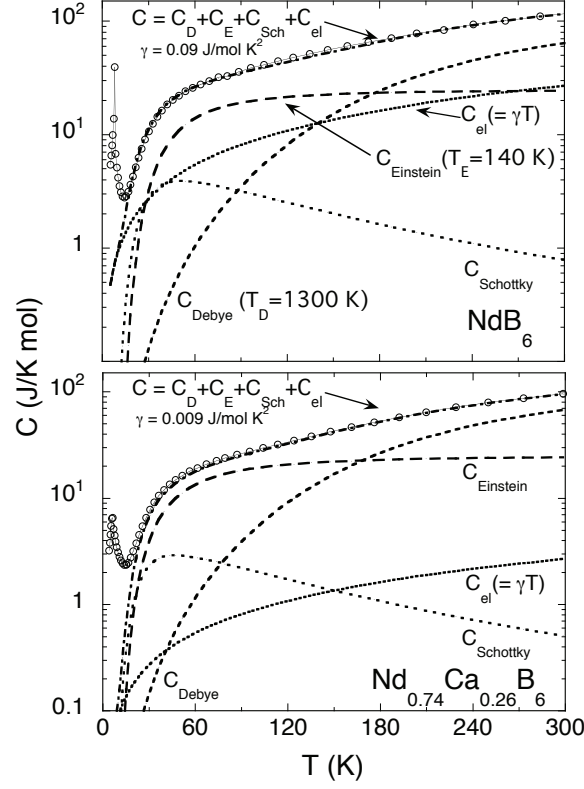


FIG. 3. Specific heat per mole of  $\text{NdB}_6$  and  $\text{Nd}_{0.74}\text{Ca}_{0.26}\text{B}_6$  vs temperature and model calculations performed as described in the text.

depend on temperature for  $\text{Nd}_{1-x}\text{Ca}_x\text{B}_6$  alloys is shown in Fig. 3. The Debye term is, as expected, very small at low temperatures, and only the Einstein contribution is significant for  $T \gtrsim 10$  K.

We now turn to the electronic and magnetic specific heat. Away from the phase transition, in the paramagnetic region,  $C_{\text{mag}} \approx C_{\text{Sch}}$ , where  $C_{\text{Sch}}$  is the Schottky contribution, brought about by the CEF splitting of the  $\text{Nd}^{+3}$  levels. This can be straightforwardly calculated from the known parameters.<sup>3-5</sup> After Ref. 5, we use a value of 100K for the first excited energy above the ground  $\Gamma_8^2$  state, and a value of 278 K for higher lying excited doublet. We then assume that the Schottky contribution scales linearly with  $x$ ; *i.e.*  $C_{\text{Sch}} = (1 - x)C_{\text{Sch}}(\text{NdB}_6)$ . To fit experimental data, we need in addition the electronic term, whose linear in  $T$  contribution is also shown in Fig. 3 for the  $x = 0$  and  $x = 0.26$  alloys. We obtain a value of  $90 \pm 10$  mJ/K<sup>2</sup>mol for  $\gamma$  in  $\text{NdB}_6$  ( $C_{\text{el}} = \gamma T$ ), in good agreement with previously reported experimental<sup>15</sup> and calculated<sup>23</sup> values. We note that this value of  $\gamma$ , in the free electron gas model, leads to an effective mass of about  $50m_e$  ( $m_e$  is the free electron

mass), which is much larger than the effective masses that follow from de Haas-van Alphen experiments.<sup>8,9</sup> It may happen that the Fermi surface is made up of two distinct sets of bands and only a FS sheet with a light mass is observed in de Haas-van Alphen experiments. Such situation has been proposed to explain a similar discrepancy in CeB<sub>6</sub>.<sup>24</sup> We also note that de Haas-van Alphen measurements are performed in high magnetic field, so the effective masses may be small.

A linear fit to the data points  $C_{el} = C(T) - C_{Sch} - C_{ph}$  in the temperature range from approximately 25 to 300 K for  $x=0$ , 0.075, and 0.264, and in the range from 25 to 40K for  $x=0.043$ , 0.124, and 0.33, gives the variation of  $\gamma(x)$  which is displayed in Fig. 4 with the corresponding error bars. The coefficient of the electronic specific heat decreases sharply upon alloying of NdB<sub>6</sub> with Ca, for  $x \lesssim 0.1$ . Our previous Hall effect measurements on Nd<sub>1-x</sub>Ca<sub>x</sub>B<sub>6</sub> showed that the carrier concentration  $n$  decreases linearly with  $x$ .<sup>25</sup> Knowing  $n$ , we can compare the value of  $\gamma(x)$  obtained from the present specific heat measurements with those expected from the Sommerfeld model of the free electron gas, in which  $\gamma = \pi^2 n k_B^2 m^* / \hbar^2 k_F^2$ . Here,  $k_B$  is the Boltzmann constant,  $m^*$  is the effective mass of carriers, and  $k_F$  is the Fermi momentum, given by  $k_F = (3\pi^2 n)^{1/3}$ , which yields the relation  $\gamma \propto m^* n^{1/3}$ . It is clear that  $\gamma(x)$  does not follow an  $n^{1/3}$  dependence, which suggests that  $m^*$  decreases non-linearly with increasing Ca content. Interestingly, the anomalous contribution to the Hall effect in Nd<sub>1-x</sub>Ca<sub>x</sub>B<sub>6</sub> single crystals shows a similar, strongly non-linear variation upon doping with Ca.<sup>25</sup> Such behavior may arise from drastic alterations of the Fermi surface upon doping.

The log-log plot of  $C(T)/T$  in the ordered state is shown in Fig. 5 for two single crystals. Below 0.6 K, the experimental heat capacity increases slightly towards 0.3 K owing to the hyperfine splitting of the Nd and B nuclei's magnetic levels.<sup>26,27</sup> We tried to fit the heat capacity in the ordered state using expressions for magnetic spin waves. However, we failed to find a reasonable fit. Solid lines in Fig. 5 show how heat capacity, arising from gapped ferromagnetic spin waves and given by  $(C - C_{hf})/T \propto T^n \exp(-\delta/k_B T)$ , where  $C_{hf}$  is the hyperfine contribution,  $k_B$  is the Boltzmann constant,  $\delta$  is the spin wave energy gap, and  $n=0.5$ ,<sup>28</sup> fits experimental points in the ordered state. The quality of the fit is poor for temperatures below 1K.

To obtain the magnetic entropy  $S$ , shown in the inset of Fig. 4, we use the relation  $S(T) = \int_0^T dT (\Delta C_{mag}/T)$ , where  $\Delta C_{mag}$  is the remainder of the total heat capacity after



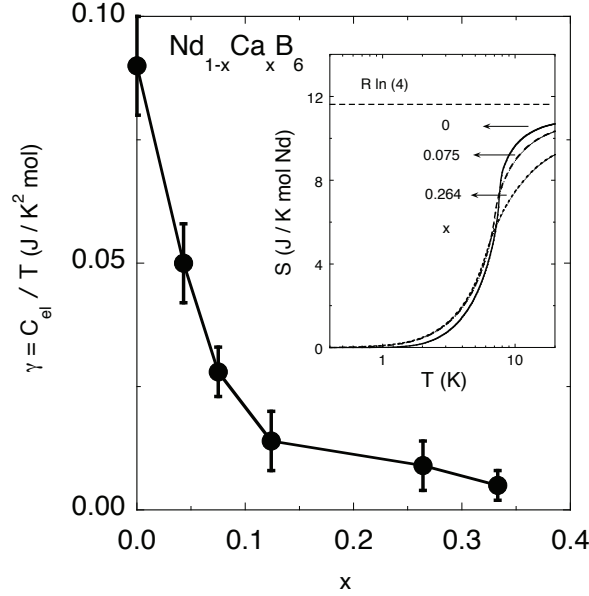


FIG. 4. Coefficient of the electronic specific heat  $\gamma$  vs content of Ca in  $\text{Nd}_{1-x}\text{Ca}_x\text{B}_6$  single crystals. The variation of magnetic entropy  $S$  vs  $T$  for some  $\text{Nd}_{1-x}\text{Ca}_x\text{B}_6$  single crystals is shown in the inset.

the hyperfine, phonon, Schottky, and electronic contributions have been subtracted. The calculated entropy is therefore associated only with the magnetic ordering. We used values of  $\gamma$  shown in Fig. 4 below  $T_N$ . This agrees with the observation that neither the number of electrons contained in the Fermi surface nor the effective mass change significantly going from the paramagnetic phase at higher temperatures to the antiferromagnetic phase at lower temperatures. Our estimate of  $S$  indicates that about 85 % of the spin entropy, associated with the ground quartet ( $R \ln(4)$ , where  $R$  is the gas constant), per mole at  $T_N$  expected for trivalent Nd is accounted for in  $x=0$ . The value of magnetic entropy at  $T_N$  agrees well with the results of earlier studies on the same system<sup>18,29</sup> and with the theoretical predictions.<sup>30</sup> Correlation ranges decrease gradually as  $T$  increases beyond  $T_N$ , and, consequently,  $S$  increases also gradually.

#### IV. CONCLUDING REMARKS

Experimentally found heat capacity of  $\text{Nd}_{1-x}\text{Ca}_x\text{B}_6$  single crystals is fitted by a simple model in which lattice and magnetic contributions are assumed to scale linearly with the

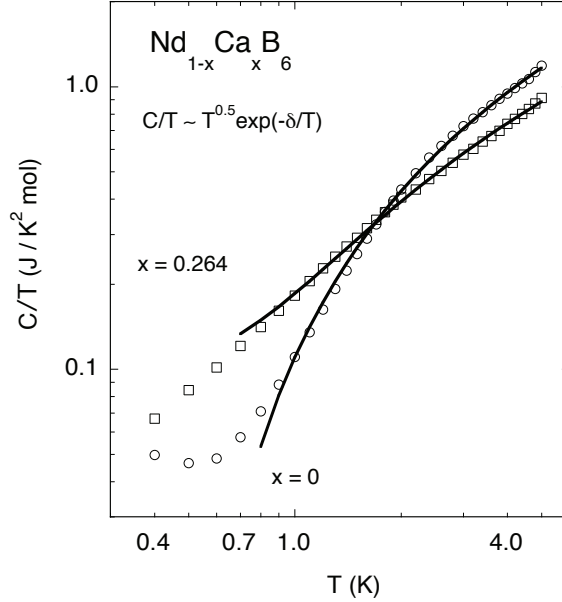


FIG. 5. Log-log plot of  $C/T$  vs  $T$  for  $\text{NdB}_6$  and  $x=0.264$  single crystals.

content of Ca. Remarkably, with the above assumption we were able to fit experimental data in a wide temperature and composition range. It shows that the  $\text{RB}_6$  structure does not deform much when a trivalent  $R$  is replaced by a divalent one, as expected for the rigid covalently-bonded boron network. Although the Raman scattering spectra of hexaborides show slight variations upon doping with divalent elements,<sup>31</sup> these seem not to affect significantly phonon and CEF parameters in alloys studied. Our results show a moderate enhancement of the electronic part in  $x = 0$  alloys both in the paramagnetic and antiferromagnetic phases. Interestingly, the low-temperature magnetic resistivity of  $\text{NdB}_6$  is also strongly enhanced with respect to the usual values of electron-magnon scattering in magnetic metals.<sup>32</sup> It points to an important role of electronic correlations in this material.

Upon doping with Ca, the electronic term in the specific heat of  $\text{Nd}_{1-x}\text{Ca}_x\text{B}_6$  in the paramagnetic phase decreases sharply, and, for  $x \gtrsim 0.1$ , shows values expected for magnetic metals. The electronic properties of hexaborides depend critically on details of the band structure in the vicinity of the  $X$  point. In  $\text{NdB}_6$ , the electron ellipsoids centered at the  $X$  point of the Brillouin zone slightly overlap and small necks are formed between them. Doping of  $\text{NdB}_6$  with a divalent element lowers the electron concentration. Consequently, the volume of the electron ellipsoids decreases and the overlap between them, as well as the interconnecting necks, may disappear. The behavior of  $\gamma$  with Ca concentration is perhaps

what one might expect if the electron ellipsoids become separated and the large value of the electronic heat capacity is coming from the Fermi surface necks. This would explain the main features of the electronic properties we have observed.

An alternative explanation would involve effects of quadrupolar interactions which are apparently important in  $\text{NdB}_6$ .<sup>4</sup> Quadrupole related effects lead to the exotic behavior found in the filled skutterudites, and, in particular, to a large electronic specific heat.<sup>33</sup> The large value of  $\gamma$  in  $\text{NdB}_6$  ( $C_{el} = \gamma T$ ) could be related to similar interactions. Then, the strain fields that arise when Ca is doped into  $\text{NdB}_6$  lift the degeneracy of the ground state quartet of the Nd ion. Quadrupole interactions are strongly reduced and, consequently,  $\gamma(x)$  decreases. Further experimental and theoretical studies would be very helpful at this point.

## V. ACKNOWLEDGMENTS

We are happy to acknowledge support from grant MAT2008/03074, from the Ministerio de Ciencia e Innovación of Spain, and from National Science Foundation grant DMR-0854781. Additional support from Diputación General de Aragón (DGA-IMANA) is also acknowledged. We thank to Dr. S. Nakatsuji and to Dr. A. D. Bianchi for growing single crystals used in this study.

---

\* jolanta@unizar.es

- <sup>1</sup> § Electronic address: jolanta@unizar.es
- <sup>2</sup> C. M. McCarthy and C. W. Tompson, J. Phys. Chem. Solids **41**, 1319 (1980).
- <sup>3</sup> M. Loewenhaupt and M. Prager, Z. Phys. B: Condens. Matter **62**, 195 (1986).
- <sup>4</sup> G. Uimin and W. Brenig, Phys. Rev. B **61**, 60 (2000).
- <sup>5</sup> M. Reiffers, J. Šebek, E. Šantavá, N. Shitsevalova, S. Gabáni, G. Pristáš, and K. Flachbart, J. Magn. Magn. Mater. **310**, e595 (2007).
- <sup>6</sup> M. Sera, S. Itabashi, and S. Kunii, J. Phys. Soc. Jpn. **66**, 548 (1997).
- <sup>7</sup> A. P. J. van Deursen, Z. Fisk, and A. R. de Vroomen, Solid State Commun. **44**, 609 (1982).
- <sup>8</sup> Y. Onuki, A. Umezawa, W. K. Kwok, G. W. Crabtree, M. Nishihara, T. Yamazaki, T. Omi, and T. Komatsubara, Phys. Rev. B **40**, 11195 (1989).
- <sup>9</sup> R. G. Goodrich, N. Harrison, and Z. Fisk, Phys. Rev. Lett. **97**, 146404 (2006).
- <sup>10</sup> A. P. J. Arko, G. Crabtree, D. Karim, F. M. Mueller, and L. R. Windmiller, Phys. Rev. B **13**, 5240 (1976)
- <sup>11</sup> B. I. Min and Y. -R. Jang, Phys. Rev. B **44**, 13270 (1991).
- <sup>12</sup> Y. Kubo, S. Asano, H. Harima, and A. Yabase, J. Phys. Soc. Jpn. **62**, 205 (1993).
- <sup>13</sup> M. Kitamura, Phys. Rev. B **49**, 1564 (1994).
- <sup>14</sup> Z. Fisk, Solid State Commun. **18**, 221 (1976).
- <sup>15</sup> N. N. Sirota, V. V. Novikov, and S. V. Antipov, Phys. Solid State **39**, 815 (1997).
- <sup>16</sup> V. V. Novikov, Phys. Solid State **43**, 300 (2001).
- <sup>17</sup> E. F. Westrum, J. T. S. Andrews, B. H. Justice, and D. A. Johnson, J. Chem. Thermodynamics **34**, 239 (2002).
- <sup>18</sup> S. Tsuji, T. Endo, S. Kobayashi, Y. Yoshino, M. Sera, and F. Iga, J. Phys. Soc. Jpn. **71**, 2994 (2002).
- <sup>19</sup> D. Mandrus, B. C. Sales, and R. Jin, Phys. Rev. B **64**, 012302 (2001).
- <sup>20</sup> Ya. I. Dutchak, Ya. I. Fedyshin, Yu. B. Paderno, and D. I. Vadets, Izv. VUZ SSSR, Fiz. **1**, 154 (1973).
- <sup>21</sup> M. K. Blomberg, M. J. Merisalo, M. M. Korsukova, and V. N. Gurin, J. Alloys Comp. **217**, 123 (1995).

- <sup>22</sup> M. M. Korusukova, V. N. Gurin, T. Lundstrom, and L. E. Tergenius, J. Less-Common Met. **117**, 73 (1986).
- <sup>23</sup> H. D. Langford, W. M. Temmerman, and G. A. Gehring, J. Phys.: Condens. Matter **2**, 559 (1990).
- <sup>24</sup> Y. Onuki, T. Komatsubara, P. H. P. Reinders, and M. Springford, Physica B **163**, 100 (1990).
- <sup>25</sup> J. Stankiewicz, A. D. Bianchi, and Z. Fisk, J. Phys.: Conf. Ser. **200**, 012192 (2010).
- <sup>26</sup> C. D. Bredl, J. Magn. Magn. Mater. **63-64**, 355 (1987).
- <sup>27</sup> A. C. Anderson, B. Holmström, M. Krusius, and G. R. Pickett, Phys. Rev. **183**, 546 (1969).
- <sup>28</sup> E. S. R. Gopal, *Specific Heat at Low Temperatures* Plenum, Inc., New York, 1966.
- <sup>29</sup> S. Kobayashi, M. Sera, M. Hiroi, N. Kobayashi, and S. Kunii, J. Phys. Soc. Japan **68**, 3407 (1999).
- <sup>30</sup> L. J. de Jongh and A. R. Miedema, Adv. Phys. **50**, 947 (2001).
- <sup>31</sup> N. Ogita, S. Nagai, N. Okamoto, M. Udagawa, F. Iga, M. Sera, J. Akimitsu, and S. Kunii, Phys. Rev. B **68**, 224305 (2003).
- <sup>32</sup> J. Stankiewicz, S. Nakatsuji, and Z. Fisk, Phys. Rev. B **71**, 134426 (2005).
- <sup>33</sup> Y. Aoki, H. Sugawara, H. Hisatomo, and H. Sato, J. Phys. Soc. Jpn **74**, 209 (2005).